Physica Scripta. Vol. T22, 79–84, 1988.

Precise Optical Spectroscopy with Ion Traps*

Wayne M. Itano, J. C. Bergquist, Randall G. Hulet, and D. J. Wineland

Time and Frequency Division, National Bureau of Standards, Boulder, Colorado 80303, U.S.A.

Received September 24, 1987; accepted October 8, 1987

Abstract

We have used stored ion methods to improve resolution and sensitivity in optical spectroscopy. Single atomic ions have been confined by electric and magnetic fields, cooled by laser radiation pressure to temperatures on the order of 1 mK, and probed spectroscopically with narrowband lasers. The absorption resonance of a single Hg^+ ion has been observed by a decrease in the transmitted light intensity. An ultraviolet transition in Hg^+ has been observed with a linewidth of only 30 kHz. Quantum jumps to and from metastable levels of Hg^+ have been observed and used to determine radiative decay rates and to infer the existence of photon antibunching. Quantum jumps have also been observed in single Mg^+ ions.

1. Introduction

Ion traps have only recently been used in obtaining high resolution optical spectra, although their advantages have been realized for a long time. Microwave spectra of trapped ions, on the other hand, have been observed with high resolution since the 1960s [1, 2]. Elsewhere in these Proceedings, G. Werth discusses some recent experiments in this area [3]. A few years ago, at the Ninth International Conference on Atomic Physics, the field of optical spectroscopy of trapped ions was reviewed [4]. At that time, the highest resolution that had been achieved in the optical domain corresponded to a linewidth of about 3 MHz at an effective wavelength of 2.1 μm [5]. In a recent experiment to be discussed later in this Paper, an ultraviolet transition was observed with a fractional resolution about three orders of magnitude better than this [6].

Some general problems which tend to limit the resolution with which optical spectra are observed are Doppler shifts, perturbations due to collisions or to electric and magnetic fields, and the limited observation time. At least in a few favorable cases, these problems can be greatly alleviated for ions stored in traps, so that we are left with the natural linewidth. For a transition with a stable lower level, the natural linewidth (in hertz) is the inverse of the mean radiative lifetime (in seconds) of the upper level, divided by 2π.

The Doppler shift is usually divided into a term which is linear in the atomic velocity, called the first-order Doppler shift, and a part which is quadratic, called the second-order Doppler shift. The high intensity and narrow frequency width of laser light sources make it possible to apply various nonlinear spectroscopic techniques, such as saturated absorption or multiphoton absorption, that cancel the effects of first-order Doppler shifts [7]. However, the second-order Doppler shift, which is a result of relativistic time dilation, still remains. For typical laboratory conditions, this shift is only about one part in 10^{12}, but in some cases, it may seriously limit the resolution or accuracy of the measurement. One example is the work of Barger *et al.* on the 657 nm transition of calcium, which has a frequency of 4.57×10^{14} Hz and a natural linewidth of 410 Hz [8]. Resonances with linewidths as small as 2 kHz were observed, but they were severely shifted and distorted by the second-order Doppler shift.

If both the first- and second-order Doppler shifts are to be reduced, the atoms must be cooled. An atomic vapor placed in a conventional refrigeration device would quickly condense on the walls of the container. But laser cooling, a method by which laser radiation pressure is used to reduce the velocities of atoms, achieves the cooling without contact with material objects [9]. The technique was proposed independently by Hänsch and Schawlow for free atoms [10] and by Wineland and Dehmelt for trapped ions [11]. Laser cooling to temperatures on the order of 1 mK has been demonstrated with some kinds of atoms and atomic ions. This reduces the second-order Doppler shifts to the level where they are presently not a problem. An atom or atomic ion of mass 100 u (unified atomic mass units) cooled to 1 mK has a second-order Doppler shift of 1.4 parts in 10^{18}.

The observed resonance linewidth cannot be much less than the inverse of the observation time. In the case of the work on calcium, the observation time was limited to about 0.3 ms by the time it took the atoms to pass through the 21 cm long resonance region [8]. In some experiments, the observation times have been increased by confining the atoms with specially coated walls or by buffer gases, but collisions with the wall or buffer gas molecules shifted and broadened the observed resonances. Ions can be trapped for long periods by electric and magnetic fields. External field perturbations of carefully chosen transition frequencies can be less than a part in 10^{15} [12, 13]. Collisions are almost entirely absent in the ultra-high-vacuum environment of an ion trap. Neutral atoms have been trapped by static magnetic fields [14–16] and by optical fields [17], but these trapped atoms have not yet been studied spectroscopically. In these traps, the fields responsible for trapping would also have perturbed the resonances.

2. Sensitive detection of ions

A single atomic ion can easily be observed by the laser-induced fluorescence of an allowed transition, once it has been cooled so that the Doppler broadening of the transition is small. In this case, a single ion may scatter as many as 10^8 photons per second. Even if only a small fraction of the photons, around 10^{-4} in typical experimental cases, are collected and counted, the fluorescence can easily be observed [18].

The apparatus used at the National Bureau of Standards

* Contribution of the National Bureau of Standards. Not subject to copyright in the U.S.

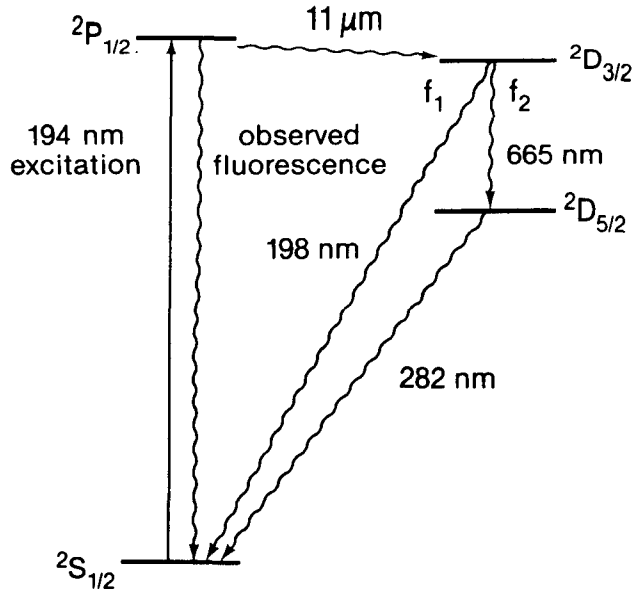

Fig. 1. The lowest energy levels of Hg^+ and the transition wavelengths. The decay rates from all three excited levels were determined by observing only the 194 nm fluorescence. (From Ref. [33]).

for experiments with Hg^+ has been described previously [19, 20]. The Hg^+ ions were confined in a radiofrequency (Paul) trap under ultra-high-vacuum conditions. In one case, a single Hg^+ ion has been kept in the trap for over a week. The lowest energy levels of Hg^+ are shown in Fig. 1. The $5d^{10}6s\ ^2S_{1/2}$ ground level is connected to the $5d^{10}6p\ ^2P_{1/2}$ level by a strong electric dipole transition. The $5d^9 6s^2\ ^2D_{3/2}$ and the $5d^9 6s^2\ ^2D_{5/2}$ levels are metastable. In order to laser cool and optically detect the ions, a few microwatts of c.w. 194 nm radiation were required. This radiation was generated by sum-frequency mixing the output of a frequency doubled 514.5 nm Ar^+ laser with the output of a 792 nm dye laser in a potassium pentaborate crystal [21]. The 194 nm fluorescence was collected by a lens system and detected by a photomultiplier tube. As many as 60 000 photons per second were detected from a single ion.

2.1. *Single-ion absorption detection*

In a recent experiment, an optical transition in a single Hg^+ ion was detected by observing the decrease in the intensity of the 194 nm beam transmitted through the trap [22]. Radio-frequency modulation techniques were used in order to avoid low frequency noise, such as that due to amplitude fluctuations of the 194 nm radiation. A maximum of about 10^{-5} of the light was absorbed. Figure 2 shows the absorption signal and the fluorescence signal, taken at the same time. The modulation and phase-sensitive detection of the absorption resulted in a signal which was approximately proportional to the frequency derivative of the fluorescence signal. Laser heating caused the fluorescence signal to drop suddenly to zero when the frequency was tuned above resonance. The integration time per point on the absorption curve was 50 s.

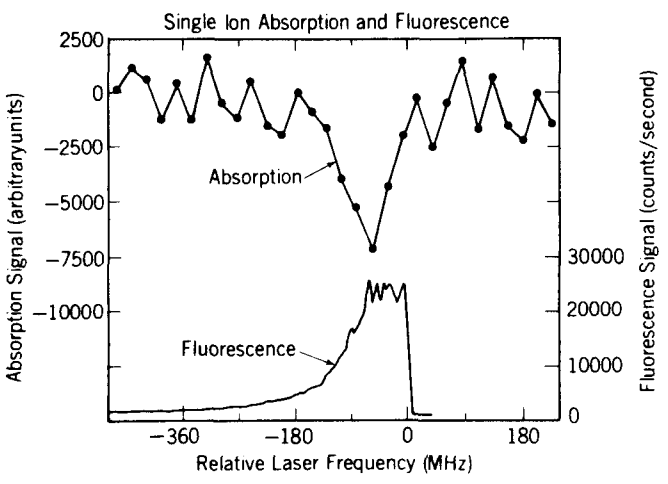

Fig. 2. The 194 nm resonance of a single Hg^+ ion due to absorption (upper trace) and fluorescence (lower trace), detected at the same time. (From Ref. [22]).

2.2. *Electron shelving*

Detecting a narrow (weakly allowed) transition by observing fluorescence from the same transition would be very difficult. A double-resonance method originally proposed by Dehmelt [23] makes it possible to detect such transitions with very high efficiency. The method can be applied to Hg^+ (see Fig. 1). The narrow, weakly-allowed, 282 nm transition is detected as follows: The ion is assumed to be initially in the ground level. Light at a wavelength near 282 nm is pulsed on, possibly driving the ion to the $^2D_{5/2}$ level. Light at a wavelength near 194 nm is then pulsed on. If the ion had made a transition in the previous step, no fluorescence would be observed; otherwise an easily detectable fluorescence signal would be observed. The method is called "electron shelving", since the optically active electron is temporarily shelved in the upper level of the weak transition.

3. Quantum jumps

The electron shelving techniques suggests a method of observing quantum jumps. If light near both resonance wavelengths is present simultaneously, then the fluorescence observed from the strong transition should turn off and on abruptly as the atom makes transitions to and from the metastable level. The dynamics of this process was investigated theoretically by Cook and Kimble [24] and later by others [25]. Quantum jumps of single ions were observed by this method in Ba^+ [26, 27], in Hg^+ [20], and recently in Mg^+ [28].

Quantum jumps have also been observed by us in Hg^+ with only the 194 nm radiation present. Once excited to the $^2P_{1/2}$ level, the ion usually decays back to the ground level, but it has a probability of about 10^{-7} to decay to the $^2D_{3/2}$ level. The probability is small because the transition frequency is low and because it requires configuration mixing to occur (the nominal configurations differ in two orbitals). From the $^2D_{3/2}$ level, the atom decays either directly to the ground level with probability f_1 or to the $^2D_{5/2}$ level with probability $f_2 = 1 - f_1$. The 194 nm fluorescence jumps between a steady level (the "on" state) when the ion is cycling between the ground level and the $^2P_{1/2}$ level and zero (the "off" state) when it is in either the $^2D_{3/2}$ level or the $^2D_{5/2}$ level.

Typical fluorescence data are shown in Fig. 3 for one, two, and three ions. The fluorescence intensity jumped from one discrete level to another and was proportional to the number of ions in the "on" state. For these data, only the 194 nm radiation was present. The intensity was high enough that quantum jumps due to the weak $^2P_{1/2}$ level to $^2D_{3/2}$ level decay occurred several times per second.

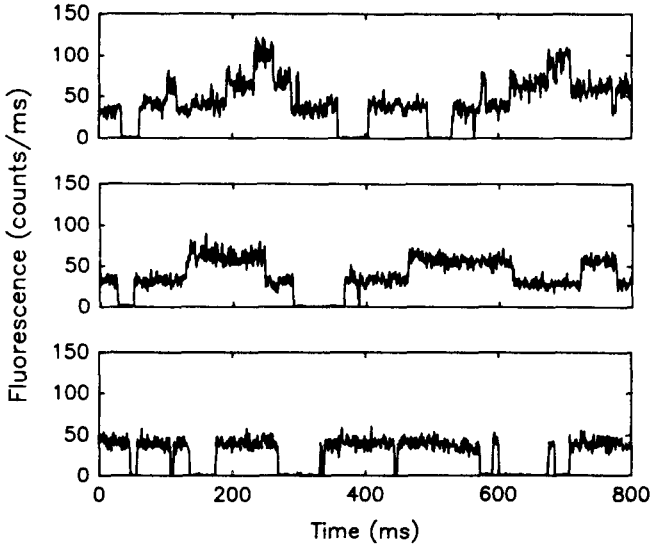

Fig. 3. Fluorescence intensities as a function of time for three Hg^+ ions (top trace), two Hg^+ ions (middle trace), and one Hg^+ ion (lowest trace). The fluorescence takes a step down when an ion makes a transition to the metastable $^2D_{3/2}$ level and takes a step up when an ion returns to the ground level from a metastable level. The integration time per point is 1 ms and the points are connected by straight lines. (From Ref. [33]).

3.1. *Quantum jumps of two and three ions*

Sauter *et al.* have reported observing multiple quantum jumps, that is, simultaneous quantum jumps of two or more ions, when several Ba^+ ions were stored in the same trap [29]. They attributed this phenomenon to a cooperative interaction between the atoms and the radiation field. We have examined our data to test the statistical independence of the quantum jumps of two or more simultaneously trapped ions.

One test was based on measuring the fractions of the time that the ions spent in each of the possible fluorescence levels. The probability distribution of fluorescence intensities was plotted for the data from one, two, and three ions. The distribution for one ion is shown in Fig. 4. The counts at low intensity (left side of plot) are due to stray scattered light when the ion is in the "off" state; the peak at high intensity (right side) is due to the fluorescence of the ion in the "on" state. The solid curve is a least-squares fit of the data to a sum of a Poisson distribution (for the left peak) and a Gaussian

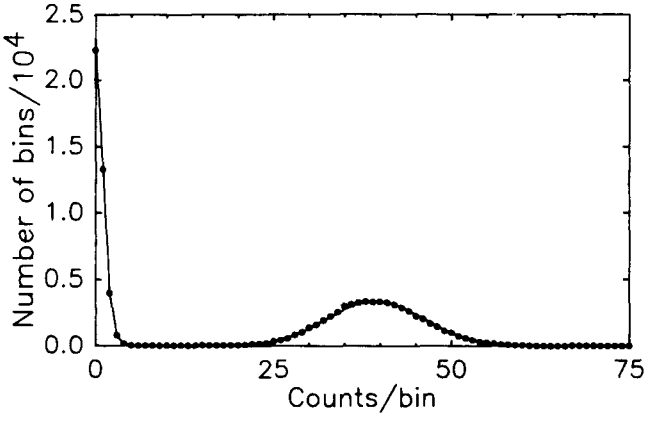

Fig. 4. Fluorescence intensity distribution for one Hg^+ ion. The numbers of 1 ms time bins in which a given number of photons was detected are plotted as dots. The solid curve is a least-squares fit to the data.

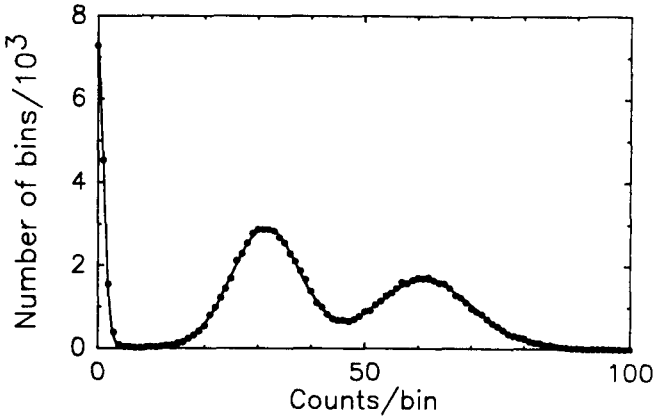

Fig. 5. Fluorescence intensity distribution for two Hg^+ ions (dots) and a least-squares fit (solid curve).

distribution (for the right peak). The standard deviation (sigma) of the fitted Gaussian is about 8% larger than the square root of the mean, which is the expected value due to statistical fluctuations. This is probably due to intensity and frequency fluctuations of the 194 nm source. The ratio of the area under the Poisson distribution to that under the Gaussian distribution is a measurement of the ratio of the time that the ion was in the "off" state to the time that it was in the "on" state (0.71 for this data set). Plots of the two-ion and three-ion intensity distributions and least-squares fits are shown in Figs. 5 and 6. The areas under the peaks of the distributions are proportional to the amounts of time that the fluorescence was at each of the various discrete levels. The curves fitted the data well, even though the peaks were not completely resolved.

Let p_{off} and p_{on} be the probabilities that a single ion is in the "off" state or the "on" state, respectively. Consider two ions subjected to the same 194 nm intensity and acting independently of each other. In this case, the probability p_0 that both are in the "off" state is equal to $(p_{off})^2$; the probability p_1 that one ion is in the "off" state and the other in in the "on" state is equal to $2p_{on}p_{off} = 2p_{on}(1 - p_{on})$; and the probability p_2 that both are in the "on" state is equal to $(p_{on})^2$. Similar relationships hold for three ions. The least-squares fit to the two-ion data yielded the values $p_0 = 0.139$, $p_1 = 0.472$, and $p_2 = 0.389$. If p_1 is (arbitrarily) chosen to calculate the value of p_{on}, then the prediction, based on the assumption of independence, is that $p_0 = 0.145$ and

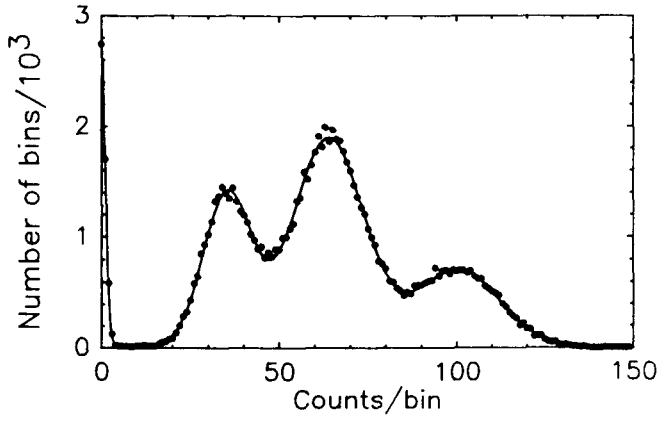

Fig. 6. Fluorescence intensity distribution for three Hg^+ ions (dots) and a least-squares fit (solid curve).

TN-152

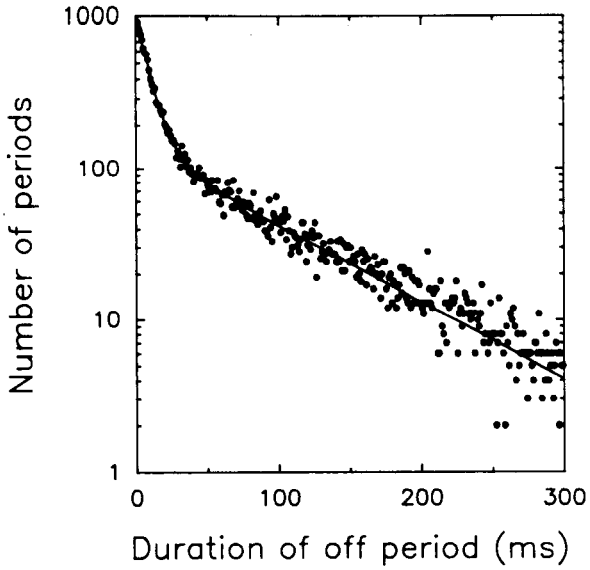

Fig. 7. Distribution of fluorescence-off periods for a single Hg^+ ion as a function of the duration of the periods (dots) and a least-squares fit. (From Ref. [33]).

$p_2 = 0.383$. For the three-ion data, let p_n ($n = 0, 1, 2, 3$) be the probability that n ions are in the "on" state. The least-squares fit yielded the values $p_0 = 0.053$, $p_1 = 0.244$, $p_2 = 0.485$, and $p_3 = 0.218$. If p_3 is used to calculate the value of p_{on}, the prediction based on independence is that $p_0 = 0.061$, $p_1 = 0.286$, and $p_2 = 0.433$. Thus, the two- and three-ion data agreed fairly well with the assumption of independence of the ions. The discrepancies from the predictions were most likely due to effects of intensity and frequency variations of the 194 nm radiation source, which are not included in the simple model used to fit the data.

In another test of independence, a search through the two-ion data was made for double quantum jumps. Over 500 consecutive jumps, which took place in a period of 20 s, were tabulated. A total of five apparent double quantum jumps were found, which is approximately the number that would be expected due to random coincidences within the finite resolving time of the instrumentation (1 ms).

3.2. *Measurements of radiative decay rates*

The radiative decay rates of the $^2D_{3/2}$ level and the $^2D_{5/2}$ level are reflected in the probability distribution W_{off} of the durations of the "off" periods for a single ion irradiated by 194 nm radiation. A calculation based on the rate equations for the probabilities of being in the various levels yields

$$W_{off}(\tau) \propto [f_2\gamma_2 \exp(-\gamma_2\tau) + (f_1\gamma_1 - \gamma_2)\exp(-\gamma_1\tau)]. \quad (1)$$

Here γ_1 and γ_2 are the total radiative decay rates of the $^2D_{3/2}$ level and the $^2D_{5/2}$ level respectively.

The experimental fluorescence-off distribution was least-squares fitted to eq. (1) to obtain values for γ_1, γ_2, and f_1. Figure 7 shows the data and the least-squares fit. The values obtained from the fit are $\gamma_1 = 109 \pm 5\,s^{-1}$, $\gamma_2 = 11.6 \pm 0.4\,s^{-1}$, and $f_1 = 0.491 \pm 0.015$. These values are in fair agreement with calculations [30, 31]. The value of γ_2 is in good agreement with previous measurements [19, 20, 32], but the value of γ_1 is about a factor of 2 higher than the only previously reported value [32]. No previous measurements of f_1 exist. The measurements will be described in more detail elsewhere [33].

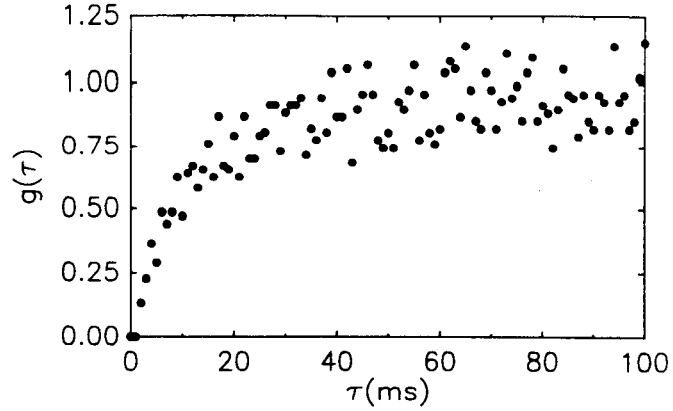

Fig. 8. Intensity correlation function of the 11 μm radiation field generated by the radiative decay from the $^2P_{1/2}$ level to the $^2D_{3/2}$ level in a single Hg^+ ion, showing the photon antibunching. The data from several runs were averaged.

3.3. *Photon antibunching*

The two-time intensity correlation function of a light field is defined by $C(\tau) = \langle I(t)I(t+\tau)\rangle$, where I is the intensity. A field is said to exhibit photon antibunching if $C(0) < C(\infty)$. No classical field can have this property, so a quantum theory is required to explain it. The quantum jumps of a single Hg^+ ion from the "on" state to the "off" state, as in the lowest trace of Fig. 3, are assumed to mark the emission of an 11 μm photon (see Fig. 1), even though these photons have not been observed directly. The probability density $g(\tau)$ that the emission of an 11 μm photon is followed a time τ later by the emission of another one is proportional to $C(\tau)$ for the 11 μm field. We expect $g(\tau)$ to go to zero for small τ, since the ion has to decay to the ground level and be excited to the $^2P_{1/2}$ level again before it can emit another 11 μm photon. The function $g(\tau)$ (normalized to 1 as $\tau \to \infty$) was calculated for several one-ion runs and averaged to obtain the graph shown in Fig. 8, which clearly shows photon antibunching. A similar graph, showing photon antibunching in the 282 nm radiation emitted when light at both 194 nm and 282 nm was applied, has been shown previously [20].

3.4. *Quantum jumps in Mg^+*

Quantum jumps of a single $^{24}Mg^+$ ion in a Penning trap were investigated recently [28]. A single 280 nm radiation source was present and was tuned close to the $m_J = -1/2$ to $m_J = -3/2$ Zeeman component of the transition from the $3s\ ^2S_{1/2}$ ground level to the $3p\ ^2P_{3/2}$ level. The fluorescence intensity dropped to zero when the ion was driven to the $m_J = +1/2$ sublevel of the ground level by a spontaneous Raman transition, and returned to its previous level when another spontaneous Raman transition drove the ion back to the $m_J = -1/2$ sublevel. A trace of the fluorescence intensity as a function of time is shown in Fig. 9. The data are in agreement with the theoretical prediction that the ratio of the time when the fluorescence is on to the time when it is off is very close to 16 [34]. This ratio is nearly independent of the 280 nm intensity because of the existence of coherences between excited levels. The experimental results provide a high precision (2%) verification of an effective two-state rate equation description of the dynamics of the quantum jumps.

TN-153

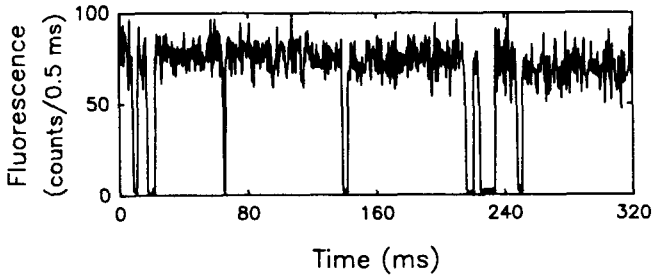

Fig. 9. Fluorescence intensity of a single Mg^+ ion as a function of time, showing the sudden changes due to quantum jumps to and from the ground-state Zeeman level which is not in resonance with the incident radiation. (Adapted from Ref. [28]).

4. Suppression of Doppler broadening by confinement

In 1953 Dicke showed that the confinement of an atom to a region smaller than the resonance-radiation wavelength leads to a suppression of the first-order Doppler shift broadening [35]. This condition is the basis for the observation of narrow Mössbauer transitions of the nuclei in solids. It is also easy to satisfy this condition, commonly called the Lamb–Dicke criterion, for a microwave resonance, since the wavelengths can be several centimeters long. Microwave frequency standards such as the atomic hydrogen maser make use of this fact. In the optical domain, it can be satisfied for a single, laser-cooled ion confined in a trap. The residual first-order Doppler broadening takes the form of discrete resonances, displaced from the unshifted central resonance (the carrier), by multiples and combinations of the frequencies of motion of the ion. These extra resonances are called motional sidebands.

4.1. *High resolution spectra of Hg^+*

We have used the shelved-electron method to detect the weak $^2S_{1/2}$ to $^2D_{5/2}$ transition of a single Hg^+ ion [6]. If the fluorescence was high enough to indicate that the ion was cycling between the $^2S_{1/2}$ and the $^2P_{1/2}$ levels, the 194 nm radiation was turned off and the 282 nm radiation was turned on for 20 ms,

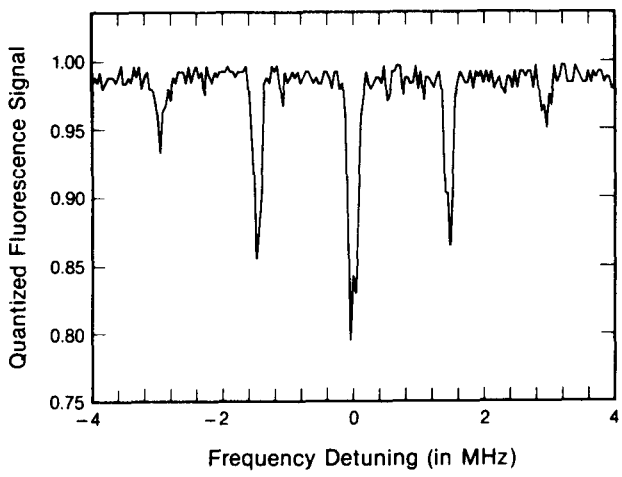

Fig. 10. The $^2S_{1/2}$ to $^2D_{5/2}$ resonance due to absorption of 282 nm radiation from a frequency-doubled dye laser by a single Hg^+ ion. The shelved electron method was used to detect this weakly allowed transition. The weaker absorption lines (motional sidebands) are separated from the central resonance by multiples of the frequencies of harmonic motion of the trapped ion and are due to the Doppler shift of the 282 nm radiation in the frame of the ion. (From Ref. [6]).

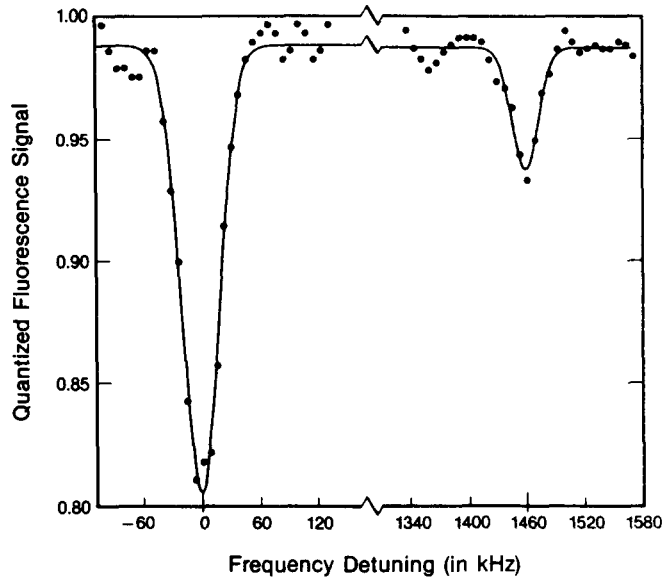

Fig. 11. High resolution frequency scan of the $^2S_{1/2}$ to $^2D_{5/2}$ resonance, showing the central resonance and the first upper motional sideband. From Ref. [6]).

which is much less than the $^2D_{5/2}$ level lifetime. The 194 nm radiation was turned on again, and the fluorescence photons were counted for 10 ms to see whether the ion had made a transition to the $^2D_{5/2}$ level. The result of the measurement was a 0 or a 1, depending on whether the number of photons detected was below or above a threshold level. This eliminated certain kinds of instrumental noise, such as intensity fluctuations of the detection laser, leaving only the inherent quantum fluctuations of the atom. Figure 10 shows a spectrum taken in the manner just described, displaying the carrier and two motional sidebands on each side. Figure 11 shows a high resolution scan of the carrier and the first upper sideband. The resonances are approximately 30 kHz wide. The ratio of intensities of the carrier and sideband indicates that the ion was cooled to near the theoretical minimum of 1.7 mK. The limit of 30 kHz resolution was due to laser frequency fluctuations. If a suitably stabilized laser were used, the resolution would approach the natural linewidth of about 2 Hz. The sensitivity of the transition frequency to fluctuations in the magnetic field could essentially be eliminated by using a suitable Zeeman component in either $^{199}Hg^+$ or $^{201}Hg^+$ [36].

Acknowledgements

We gratefully acknowledge the support of the Air Force Office of Scientific Research and the Office of Naval Research.

References

1. Dehmelt, H., Adv. At. Mol. Phys. **3**, 53 (1967); *ibid*, **5**, 109 (1969).
2. Wineland, D. J., Itano, W. M. and Van Dyck, Jr., R. S., Adv. At. Mol. Phys. **19**, 135 (1983).
3. Werth, G., these Proceedings.
4. Wineland, D. J., Itano, W. M., Bergquist, J. C., Bollinger, J. J. and Prestage, J. D., Atomic Physics 9 (Edited by R. S. Van Dyck, Jr. and E. N. Fortson), p. 3. World Scientific, Singapore, 1985.
5. Janik, G., Nagourney, W. and Dehmelt, H., J. Opt. Soc. Am. B **2**, 1251 (1985).
6. Bergquist, J. C., Itano, W. M. and Wineland, D. J., Phys. Rev. A **36**, 428 (1987).

7. High-Resolution Laser Spectroscopy (Edited by K. Shimoda). Springer Verlag, Berlin, 1976; Levenson, M. D., Introduction to Nonlinear Laser Spectroscopy. Academic Press, New York, 1982.
8. Barger, R. L., Bergquist, J. C., English, T. C. and Glaze, D. J., Appl. Phys. Lett. **34**, 850 (1979); Barger, R. L., Opt. Lett. **6**, 145 (1981).
9. Wineland, D. J. and Itano, W. M., Phys. Today **40**, 34 (June 1987).
10. Hänsch, T. W. and Schawlow, A. L., Opt. Commun. **13**, 68 (1975).
11. Wineland, D. J. and Dehmelt, H., Bull. Am. Phys. Soc. **20**, 637 (1975).
12. Dehmelt, H. G., IEEE Trans. Instrum. Meas. **IM-31**, 83 (1982).
13. Wineland, D. J., Science **226**, 395 (1984).
14. Migdall, A. L., Prodan, J. V., Phillips, W. D., Bergeman, T. H. and Metcalf, H. J., Phys. Rev. Lett. **54**, 2596 (1985).
15. Bagnato, V. S., Lafyatis, G. P., Martin, A. G., Raab, E. L., Ahmad-Bitar, R. N. and Pritchard, D. E., Phys. Rev. Lett. **58**, 2194 (1987).
16. Hess, H. F., Kochanski, G. P., Doyle, J. M., Masuhara, N., Kleppner, D. and Greytak, T. J., Phys. Rev. Lett. **59**, 672 (1987).
17. Chu, S., Bjorkholm, J. E., Ashkin, A., and Cable, A., Phys. Rev. Lett. **57**, 314 (1986).
18. Neuhauser, W., Hohenstatt, M., Toschek, P. E. and Dehmelt, H., Phys. Rev. **A22**, 1137 (1980).
19. Bergquist, J. C., Wineland, D. J., Hemmati, H., Daniel, H.-U. and Leuchs, G., Phys. Rev. Lett. **55**, 1567 (1985).
20. Bergquist, J. C., Hulet, R. G., Itano, W. M. and Wineland, D. J., Phys. Rev. Lett. **57**, 1699 (1986).
21. Hemmati, H., Bergquist, J. C. and Itano, W. M., Opt. Lett. **8**, 73 (1983).
22. Wineland, D. J., Itano, W. M. and Bergquist, J. C., Opt. Lett. **12**, 389 (1987).
23. Dehmelt, H. G., Bull. Am. Phys. Soc. **20**, 60 (1975).
24. Cook, R. J. and Kimble, H. J., Phys. Rev. Lett. **54**, 1023 (1985).
25. Javanainen, J., Phys. Rev. **A33**, 2121 (1986); Schenzle, A., DeVoe, R. G. and Brewer, R. G., Phys. Rev. **A33**, 2127 (1986); Cohen-Tannoudji, C. and Dalibard, J., Europhys. Lett. **1**, 441 (1986); Pegg, D. T., Loudon, R. and Knight, P. L., Phys. Rev. **A33**, 4085 (1986); Schenzle, A. and Brewer, R. G., Phys. Rev. **A34**, 3127 (1986); Kimble, H. J., Cook, R. J., and Wells, A. L., Phys. Rev. **A34**, 3190 (1986); Zoller, P., Marte, M. and Walls, D. F., Phys. Rev. **A35**, 198 (1987); Nienhuis, G., Phys. Rev. **A35**, 4639 (1987); Porrati, M. and Putterman, S., Phys. Rev. **A36**, 929 (1987).
26. Nagourney, W., Sandberg, J. and Dehmelt, H., Phys. Rev. Lett. **56**, 2797 (1986).
27. Sauter, Th., Neuhauser, W., Blatt, R. and Toschek, P. E., Phys. Rev. Lett. **57**, 1696 (1986).
28. Hulet, R. G., Wineland, D. J., Bergquist, J. C., and Itano, W. M., (submitted for publication)
29. Sauter, Th., Neuhauser, W., Blatt, R. and Toschek, P. E., Opt. Commun. **60**, 287 (1986).
30. Garstang, R. H., J. Res. Natl. Bur. Stand. Sect. **A68**, 61 (1964).
31. Al-Salameh, D. and Silfvast, W., AT&T Bell Laboratories, Holmdel, NJ, unpublished calculations.
32. Johnson, C. E., Bull. Am. Phys. Soc. **31**, 957 (1986).
33. Itano, W. M., Bergquist, J. C., Hulet, R. G. and Wineland, D. J., Phys. Rev. Lett. (in press).
34. Hulet, R. G. and Wineland, D. J., Phys. Rev. A **36**, 2758 (1987).
35. Dicke, R. H., Phys. Rev. **89**, 472 (1953).
36. Wineland, D. J., Itano, W. M., Bergquist, J. C. and Walls, F. L., in Proc. 35th Annual Symposium on Frequency Control, p. 602. Electronic Industries Association, Washington, D.C., 1981.

TN-155